Geometry of bee cells rediscovered

Dusan Vallo, Viliam Duris, Lucia Rumanova
dvallo@ukf.sk, vduris@ukf.sk, lrumanova@ukf.sk
Department of Mathematics Faculty of Natural Sciences
Constantine the Philosopher University in Nitra
949 01 Nitra
Slovakia

Abstract

In our paper we focus on studying the hexagonal structure of single bee cells as a mathematical modeling problem via interactive geometry software Cabri 3D and computer algebra system Maple®6. We derive the functions which describe the surface area for both mathematical models and determine extremes of the surface area functions using calculus. The extremes obtained from the mathematical models are also contrasted with experimental data obtained by beekeeping experts.

1 Introduction

The famous historical problem of honeycomb elegance and the geometry of a single bee cell as a solid called rhombic dodecahedron has fascinated many mathematicians and scientists. The essence of the problem has been explored from different perspectives, from the strictly scientific and philosophical to the educational.

Hope-Jones [1] has written that: *„This interesting solid has tended too much in the past to be classified as for adults only (and for not too many of them), but because it supplies the answer to a question which every intelligent youngster asks himself I think it is worthwhile to try and smooth the path of any teacher who wants to let children of (say) 13 share in some of its treasure."*

The topic is not original, but since antiquity the shape of a bee cell has resulted in many interesting investigations like the great geometry problem of how to tesselate a space with convex congruent polyhedra. In this paper, we show how technology facilitates modeling to make the mathematical problem of the shape of a bee cell more accesible. With reference to [2], we derive functions describing the surface area for two models, which are based on a rhombic dodecahedron and a snub octahedron. The use of calculus in finding the extrema of both functions will be necessary. One can observe that a more complex model corresponds to a complicated expression of function, in which finding a minimum requires using software with an implemented computer algebra system.

1.1 The geometry of a bee cell: a short historical overview

As early as ancient times, the Egyptians admired the hexagonal honeycomb structure. Later on, it was Pappus of Alexandria (ca. 300 A. D.) who was fascinated by this construction and attributed the hexagonal tessellation to reasons of economy or saving. [3, 4] He saw the latent cause in the fact that only three regular polygons tile the plane: an equilateral triangle, a square and a hexagon. The hexagon encloses the largest area for the prescribed perimeter. [5] J. Kepler (1571-1630) assumed that natural powers are responsible for the structure of forms in the universe. Kepler's interest in Plato's atomic theory was transferred to his study of regular geometric structures on the growth of such things as snowflakes, pomegranates, or honeycombs. He assumed that the regular patterns of these objects could be explained by efficient packing of spheres arranged in a hexagonal lattice. Kepler predicted that this sphere's arrangements in cubes can expand into hexagonal structures so-called rhombic dodecahedra and the hexagonal cross-section of a honeycomb can be considered such a consequence of internal pressures in tight packing of wax tubes built by bees.[6] The famous French scientist Rèaumur (1683-1757) contacted many mathematicians of his time with a request to expound a mathematical solution to the problem. Explanations were given by two mathematicians - the German mathematician J. S. Koenig (1712-1757) and, independently of him, the Croatian Jesuit R. J. Boscovich (1711-1787). According to Rèaumur's claim, Koenig gave the solution in which he supposed a pyramidal roof of the bee cell. Boscovich found the errors in his logical thinking. By using calculus and methods of descriptive geometry he gave two solutions in which he proved these facts - an existence of rhombi in the cell's bottom and the equality of the spatial angles between the faces. [5]. However, the mathematical nature of the problem appeared again in 1952, when the authors Hilbert and Cohn-Vossen provided arguments for the hexagonal arrangement as the best one of greatest density. [7]

In [8], the author Thompson discusses the effects of pressure on cylindrical wax tubes. The pressure applied to a tube stored in layers is a precondition to their hexagonal arrangement. From the mathematical point of view, the hexagonal tessellation just like the bases of bee cells is not accidental. In [9] is proved that among all polygons which tile the plane the regular hexagon has the largest isoperimetric quotient, that is, has the largest area for a given perimeter.

The regularity of bee cells was analysed in more detail by Fejes-Toth in [2]. The author concentrated on honeycombs which can consist of standard bee cells or of new shapes of notional ones. The point is that the single bee cell is not a hexagonal prism. The bottom of a standard bee cell is composed of three copies of the congruent rhombi not lying in one plane, while the bottom of the hypothetical new one consists of two rhombi and two hexagons.

In this paper we explore more general constructions based on those of Fejes-Toth and we will show, using calculus, that the specific constructions found by Fejes-Toth are optimal.

2 The geometry of a bee cell

Suppose that bees need to build some type of container consisting of a lot of regular hexagonal prisms. The container is built from wax, provided that only a minimum of amount of wax will be used. This implies minimizing the ratio of the surface area to the volume of a single prism (the area of the bases of the prism are not included in the calculation). Thus, it is the same as minimizing the perimeter of the base of a single prism to its area. In [9] author has shown that even when irregular tessellating polygons are considered, the regular hexagon is best. Now we validate a subset of the Niven result.

If we consider only the regular $n-$gons, $n \geq 3$, with perimeter P_n, area A_n inscribed in a unit circle, than for the ratio it holds true that

$$\frac{P_n}{A_n} = \frac{2n.\sin\frac{\pi}{n}}{\frac{n}{2}.\sin\frac{2\pi}{n}} = \cdots = \frac{2}{\cos\frac{\pi}{n}}.$$

The sequence $\left(\frac{2}{\cos\frac{\pi}{n}}\right)_{n=3}^{\infty}$ is decreasing. The plane can be tessellated by an equilateral triangle, a square or a regular hexagon.

We will next consider a single bee cell. The cell's base will be an open regular hexagon and we will not take its area into consideration.

The rigorous view inside the real bee cells shows that a single real bee cell is not a hexagonal prism with a planar bottom. The bottom is part of the rhombic dodecahedron and consists of three congruent rhombi. These rhombi tessellate the specific zig-zagged surface. In Fig. 1 we demonstrate a constitution of polyhedra which represent the top part of bee cells by using the software Cabri 3D.

Let $A_0B_0C_0D_0E_0F_0$ be any given regular hexagon in an original plane. The centre of the hexagon is denoted S_0. A line o, which is perpendicular to the original plane, and pass through the point S_0, is called axis o.

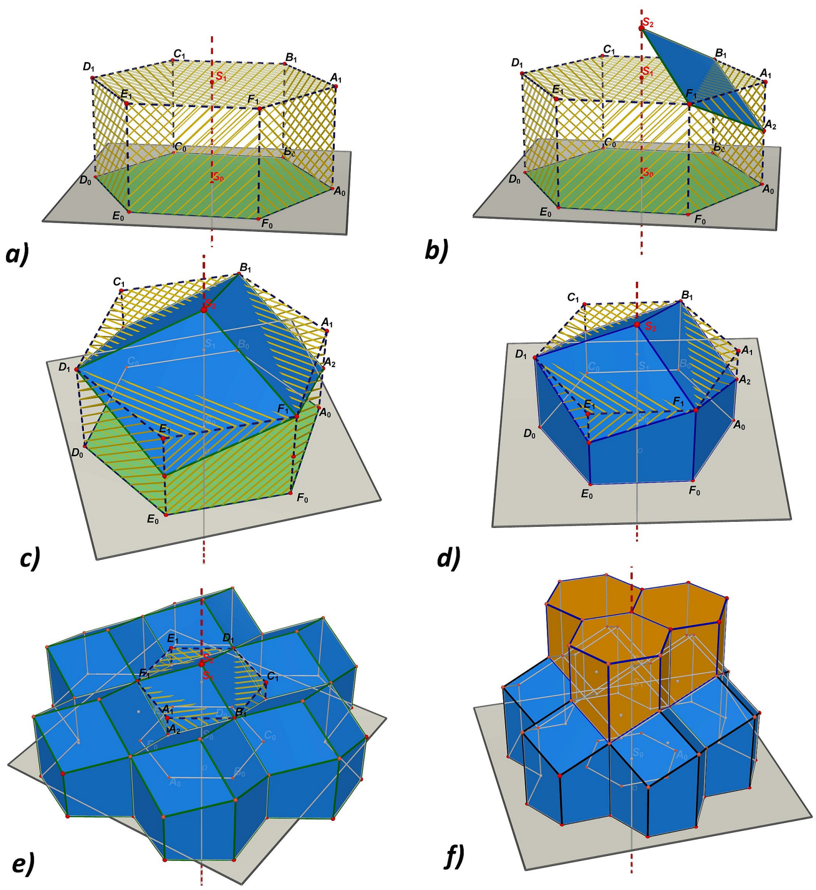

Figure 1: The formation of polyhedron which represents a single bee cell (Fig. 2a - d) and a consecutive composition of ten bee cells in honeycomb (Fig. 2e - f).

In Fig. 2a, regular hexagon $A_0B_0C_0D_0E_0F_0$ represents a cross-section of a bee cell. The right prism with height S_0S_1 and this hexagon as a base has been constructed. The rhombus $S_2F_1A_2B_1$ has been constructed in a condition that the point S_2 lies on line o and holds $S_1S_2 = A_1A_2$ (see Fig. 2b). In Fig. 2c, the rhombi $S_2B_1C_2D_1$ and $S_2D_1E_2F_1$ has been similarly constructed. In Fig. 2d, the polyhedron represents the top part of a bee cell with its top composed of three congruent rhombi. In the case that $D_1F_1 = \sqrt{2}S_2E_2$ the three rhombi form part of a rhombic dodedahedron. The polyhedra in Fig. 2e represent the top part of seven cells. These also form the bottom of three cells, as illustrated in Fig. 2f.

2.1 The mathematical model of a standard bee cell

The first observation by using Cabri 3D is related to the volume of a single bee cell. Let us consider points S_1 and A_1 as perpendicular projections of the points S_0 and A_0 on the original plane. Holds that $S_0S_1 = x = A_0A_1$.

The volumes of rectangular tetrahedrons $B_0F_0A_1A_0$ and $B_0F_0S_1S_0$ are equal (tetrahedrons have congruent bases $B_0F_0A_1$, $B_0F_0S_1$ and the same height x). An analogical situation is in cases when we consider two other pairs of tetrahedrons, e.g. $B_0D_0C_1C_0$, $B_0D_0S_1S_0$. The software Cabri 3D provides calculations of the volumes directly (see Fig. 2). Let's evaluate the volume and surface area of a single cell by using Cabri 3D software. We observe that by increasing the distance x, the value of the surface area is changed. We also explore that for the specific distance x, the value of the area surface is a minimum.

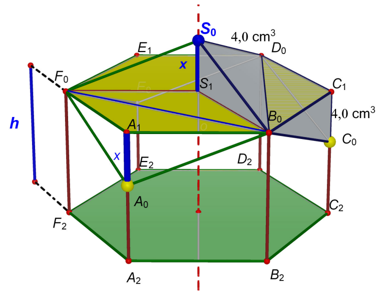

Figure 2: The mathematical model of a single bee cell by using Cabri 3D. The volume of the cell is independent of x.

Remark 1 *We use Cabri 3D tools (Manipulation, Area, Volume and Calculator) to evaluate the surface area and the volume of the model. The displayed value of the surface area corresponds to the values of e, h. We recall that we deal with an open cell, that is, the area of its hexagonal cap $A_2B_2C_2D_2E_2F_2$ is not counted.*

The extreme value for the surface area is connected with one of the internal angles of the rhombus at approximately $109°$. To determine the exact values for the extreme, we derive the function $p(x)$ of the surface area of the model cell with a variable x and parameters $e = A_2B_2, h = F_0F_2$ (label e means edge; h means height). The rhombus $A_0B_0S_0F_0$ has diagonals A_0S_0, B_0F_0. The diagonal B_0F_0 is diagonal in the hexagon $A_1B_0C_1D_0E_1F_0$ in the original plane.

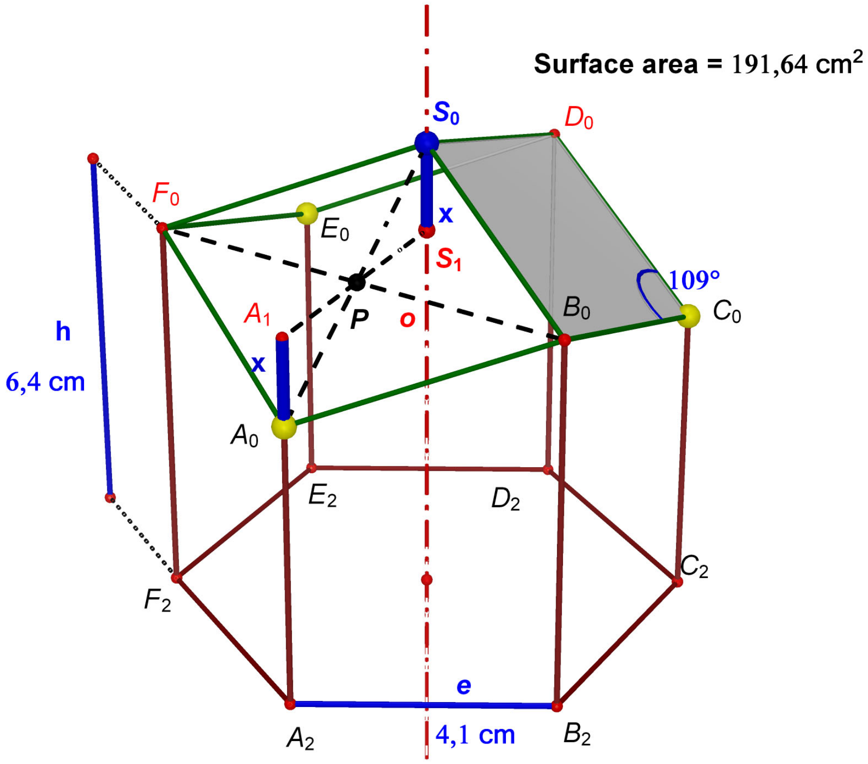

Figure 3: Evaluation of the surface area of a bee cell, lengths of edges A_2B_2 , F_0F_2, distance $x = S_0S_1$ and one of an internal angle of congruent rhombi.

Using the law of cosines for the sides of the triangle $F_0B_0A_1$ we calculate that $B_0F_0 = e\sqrt{3}$. It is evident that the segment A_1S_1 has a length of e. If we label P a midpoint of A_1S_1, then from the Pythagorean Theorem we derive

$$A_0P = \frac{\sqrt{4x^2 + e^2}}{2} \tag{1}$$

that implies

$$A_0S_0 = \sqrt{4x^2 + e^2}. \tag{2}$$

The area of the rhombus $A_0B_0S_0F_0$ is

$$A_r = \frac{\sqrt{3}}{2} e\sqrt{4x^2 + e^2}. \tag{3}$$

The area of the trapezoid $A_2B_2B_0A_0$ is

$$A_t = eh - \frac{1}{2}xe = \frac{e}{2}(2h - x). \tag{4}$$

The surface of the model cell is comprised of three rhombi and six trapezoids. The exact expression of the function $p(x)$ is

$$p(x) = 3e\left(\frac{\sqrt{3(4x^2 + e^2)}}{2} + 2h - x\right). \tag{5}$$

We will use the first-derivative test and it holds true that

$$p'(x) = 3e\left(\frac{2\sqrt{3}x}{\sqrt{4x^2+e^2}} - 1\right). \tag{6}$$

Setting $p'(x) = 0$ and solving for $x > 0$, we easily find

$$x_0 = e\frac{\sqrt{2}}{4}. \tag{7}$$

The second-derivative test tells us that for all real x it holds true that

$$p''(x) = 3e\left(\frac{2\sqrt{3}.\sqrt{4x^2+e^2} - 2\sqrt{3}x.\frac{8x}{2\sqrt{4x^2+e^2}}}{\left(\sqrt{4x^2+e^2}\right)^2}\right)$$

$$p''(x) = \frac{6\sqrt{3}e^3}{\left(\sqrt{4x^2+e^2}\right)^3} > 0 \tag{8}$$

The function (5) has a local minimum at $x_0 = e\frac{\sqrt{2}}{4}$. The parameter h has no impact on the critical number (7). On the other hand, the length of the edge e does not affect the internal angles in the model because two similar shapes have congruent corresponding angles. Let us calculate the internal angles in the rhombus $A_0B_0S_0F_0$.
First we evaluate the length of the diagonal A_0S_0 . Substituting $x = e\frac{\sqrt{2}}{4}$ in (2) we obtain

$$A_0S_0 = e\sqrt{\frac{3}{2}}. \tag{9}$$

Now, in the triangle A_0B_0P we use the tangent function for $\varphi = \angle B_0A_0F_0$ and it holds true that

$$\tan\frac{\varphi}{2} = \frac{PB_0}{PA_0}. \tag{10}$$

Substituting $PB_0 = e\frac{\sqrt{3}}{2}$ and $PA_0 = \frac{e}{2}\sqrt{\frac{3}{2}}$, we find

$$\tan\frac{\varphi}{2} = \sqrt{2}. \tag{11}$$

This implies that

$$\varphi \doteq 109.47° \tag{12}$$

and for $\psi = \angle A_0B_0S_0$ we evaluate

$$\psi = 180° - \varphi = 70.53°. \tag{13}$$

The angle $\angle B_0A_0A_2 = \omega$ in the trapezoid $B_0A_0A_2B_2$ is an adjacent angle in the triangle $A_0B_0A_1$ at a vertex A_0 and it holds true that

$$\tan(180° - \omega) = \frac{A_1B_0}{A_1A_0}. \tag{14}$$

Substituting $A_1B_0 = e$ and $A_1A_0 = x = e\frac{\sqrt{2}}{4}$, we find

$$\omega \doteq 109.47°. \tag{15}$$

From (12) and (15), it is evident that the planar angles at vertices A_0, C_0, E_0, are equal. This implies that the three rhombi form a part of rhombic dodecahedron.

2.2 The second model of the bee cell

Obviously, the results described above are incredible; among all open cells of constant volume which can be based on the hexagonal honeycomb structure we can find the surface with the least area. [4] In the paper [2] the author describes a special construction of such polyhedron. The idea of the construction is based on the truncations of the corners of irregular octahedron. The final parallelohedron is illustrated in Fig. 4

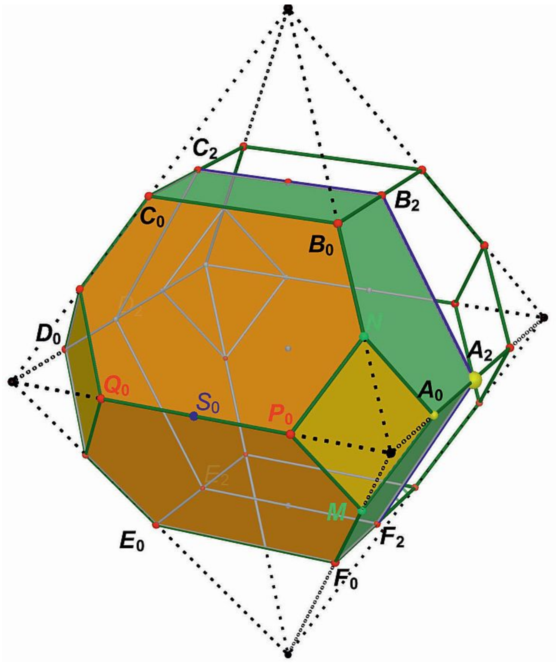

Figure 4: The Fejes-Toth construction of the irregular truncated octahedron. The indicated cross-section $A_2B_2C_2D_2E_2F_2$ is regular hexagon. Its center is a point of symmetry of this polyhedron. The polyhedron consists from two squares, eight irregular hexagons and four rhombi. In accordance with Fejes-Toth's construction holds true that $B_0C_0Q_0P_0$ is square, too. In notation $A_2B_2 = s$ holds true that $MP_0 = \frac{\sqrt{5}}{4}s$, $MN = \frac{\sqrt{3}}{2}s$ and $A_0P_0 = \frac{\sqrt{2}}{2}s$.

Fejes-Toth proved that in a condition of the congruent hexagonal cross-section of the polyhedra and their equal volumes the cell arising from the truncated octahedron has a smaller surface-area than the cell based on the rhombic dodecahedron. In his article with the exciting title *What the Bees Know and What They Do Not Know*, the author writes that: *,,Instead of closing the bottom of a cell by three rhombi, as the bees do, it is always more efficient to use two hexagons and two rhombi"*.
Next we will investigate a mathematical model of the shape based on a snub octahedron. Using calculus, we will find the extrema of the surface-area function of the cell.
First, we construct the model by using Cabri 3D software.

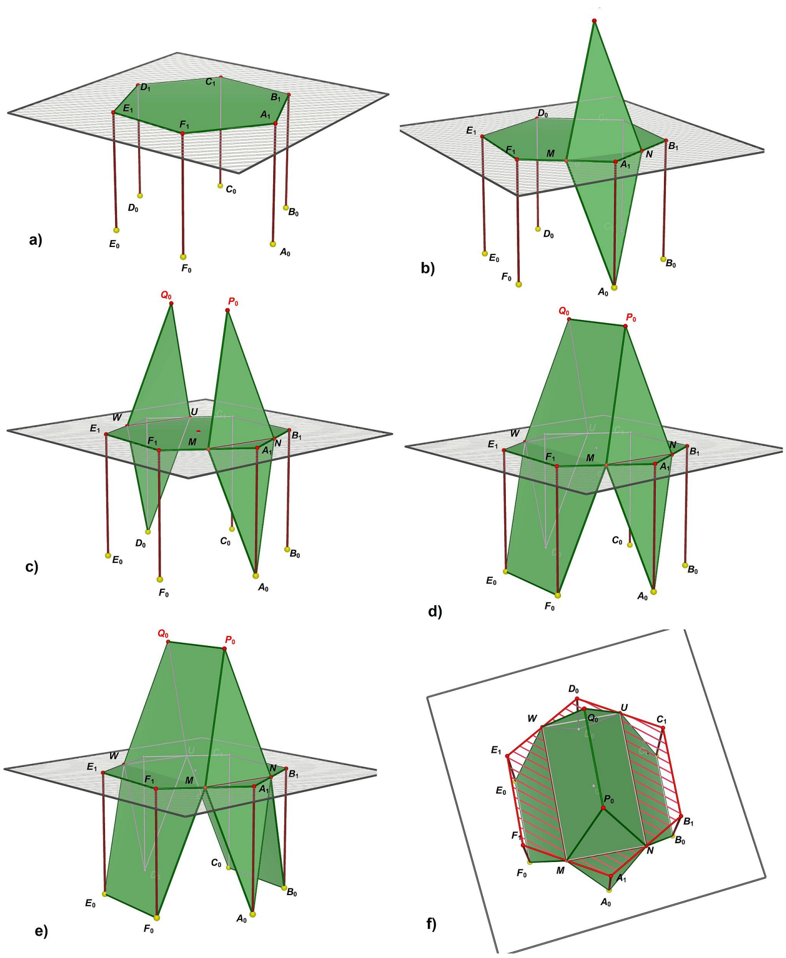

Figure 5: The sequence of smaller figures which give stages in construction of the single bottom.

If $A_1B_1C_1D_1E_1F_1$ is the fundamental hexagon in the original plane, then only midpoints M, N, U, W of the sides A_1F_1, A_1B_1, C_1D_1, D_1E_1 are incident to the original plane. If we put our attention on a single cell whose fundamental hexagon $A_1B_1C_1D_1E_1F_1$ is incident to the original plane, then the bottom is folded up from two rhombi A_0NP_0M, D_0UWQ_0 and two hexagons $B_0C_0UQ_0P_0N$, $F_0MP_0Q_0WE_0$.
It is evident that the model and the hexagonal prism have equal volumes. If points P_1, Q_1 are perpendicular projections of the points P_0, Q_0 onto the original plane, then tetrahedrons MNA_1A_0, MNP_1P_0 are congruent. Oblique triangular prisms $NUC_0B_0B_1C_1$, $NUQ_0P_0P_1Q_1$ are congruent, too. The particular situation is demonstrated in Fig. 6

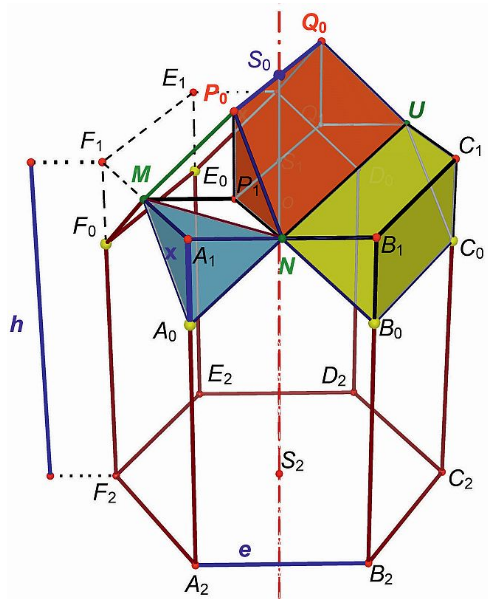

Figure 6: Demonstration of equal volumes for the hexagonal prism and the model of the cell.

Let us evaluate a surface area of the model by using Cabri 3D software. We observe that with an increasing distance x the area of the surface is changed and for the specific distance x (see Fig. 7).

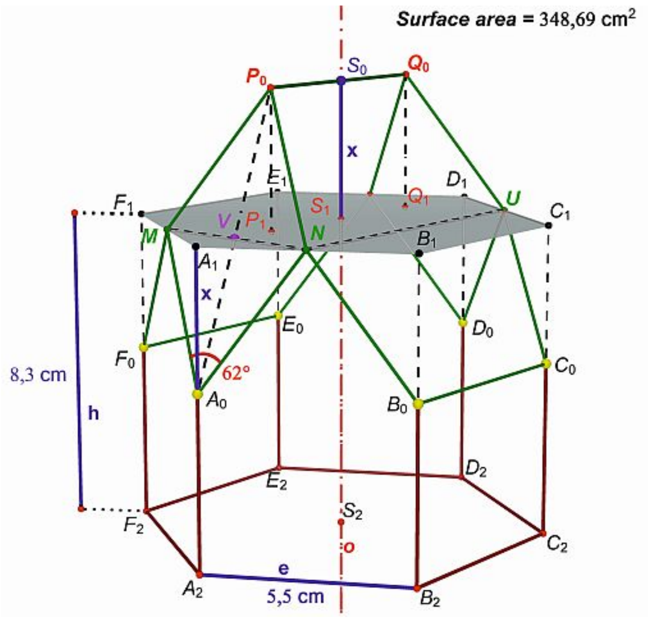

Figure 7: Evaluation of the surface area of the model with respect to the parameters e, h (calculated with Cabri 3D).

We derive the function $q(x)$ with an variable x, which will determine the surface area of the model.

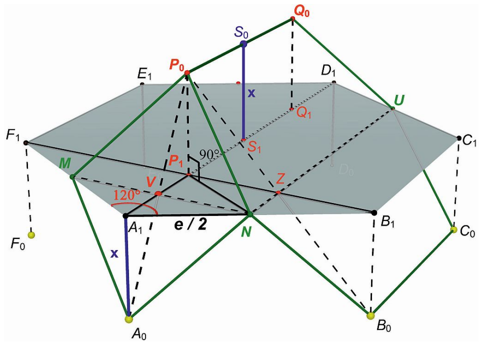

Figure 8: The geometric details of the model. It also holds true that the points P_1, Q_1 are midpoints of the segments A_1S_1, S_1D_1.

Using the law of cosines for the sides of the triangle $F_1B_1A_1$ we obtain

$$F_1B_1 = e\sqrt{3} \tag{16}$$

this implies

$$MN = e\frac{\sqrt{3}}{2}. \tag{17}$$

If V is a midpoint MN, then we determine the length of A_1V by using a tangent function in right-angled triangle A_1NV. Holds

$$\tan 60^\circ = \frac{\frac{MN}{2}}{A_1V}. \tag{18}$$

This implies that

$$A_1V = \frac{e}{4}. \tag{19}$$

Using the Pythagorean Theorem in the triangle A_0VA_1, we derive

$$A_0V = \frac{\sqrt{16x^2 + e^2}}{4} \tag{20}$$

and it holds true that

$$A_0P_0 = \frac{\sqrt{16x^2 + e^2}}{2}. \tag{21}$$

The area of the rhombus A_0NP_0M is

$$A_r = e\frac{\sqrt{3}}{8}\sqrt{16x^2 + e^2}. \tag{22}$$

Now, we derive a formula for the area of the hexagon $B_0C_0UQ_0P_0N$. The segment P_1N is midline segment in the triangle $A_1B_1F_1$ and it holds true that

$$P_1N = \frac{e}{2} \tag{23}$$

From the rectangular triangle P_0NP_1 we derive

$$P_0N = \frac{\sqrt{4x^2+e^2}}{2}. \tag{24}$$

The segment NU is a midline segment in the trapezoid $A_1D_1C_1B_1$ and holds true that

$$NU = \frac{A_1D_1 + B_1C_1}{2} = \frac{3}{2}e. \tag{25}$$

If we consider a point Z, the intersection between F_1B_1 and NU, then the segment P_0Z is an altitude to the trapezoid NP_0Q_0U and holds true that $P_1Z = \frac{F_1B_1}{4}$. From Pythagoras Theorem on triangle P_0P_1Z implies that

$$P_0Z = \frac{\sqrt{16x^2+3e^2}}{4}. \tag{26}$$

The area of the hexagon $B_0C_0UQ_0P_0N$ is

$$A_h = 2\frac{P_0Q_0 + NU}{2} \cdot P_0Z, \tag{27}$$

$$A_h = e\frac{5\sqrt{16x^2+3e^2}}{8}. \tag{28}$$

Now, we derive formulas for the surface area of the lateral faces of the model.
The area of the pentagon $A_2B_2B_0NA_0$ is

$$A_p = h.e - 2 \cdot \frac{e.x}{4} = h.e - \frac{e.x}{2}. \tag{29}$$

The area of the rectangle $B_2C_2C_0B_0$ is

$$A_{re} = e\left(h - x\right). \tag{30}$$

Finally, for the surface area of the model (without the hexagonal base) it holds true that

$$q\left(x\right) = 2 \cdot A_r + 2 \cdot A_h + 4 \cdot A_p + 2 \cdot A_{re} \tag{31}$$

and we obtain

$$q\left(x\right) = 2 \cdot e\frac{\sqrt{3}}{8}\sqrt{16x^2+e^2} + 2 \cdot e\frac{5\sqrt{16x^2+3e^2}}{8} + 4 \cdot \left(h.e - \frac{e.x}{2}\right) + 2 \cdot e\left(h - x\right). \tag{32}$$

After simplification

$$q\left(x\right) = 2 \cdot e\left(\frac{\sqrt{48x^2+3e^2} + 5\sqrt{16x^2+3e^2}}{8} + 3h - 2x\right), \tag{33}$$

where $e = A_2B_2, h = F_1F_2$ are parameters.

How can we find an extreme?
If we use the first-derivative test and put $q'(x) = 0$ for $x > 0$, then we derive an algebraic equation involving surds. This equation requires special consideration because it is in eight degree after a simplification.
In this situation we help ourselves with a computer algebra system included in Maple®6 software. Its application is presented in Fig. 9.

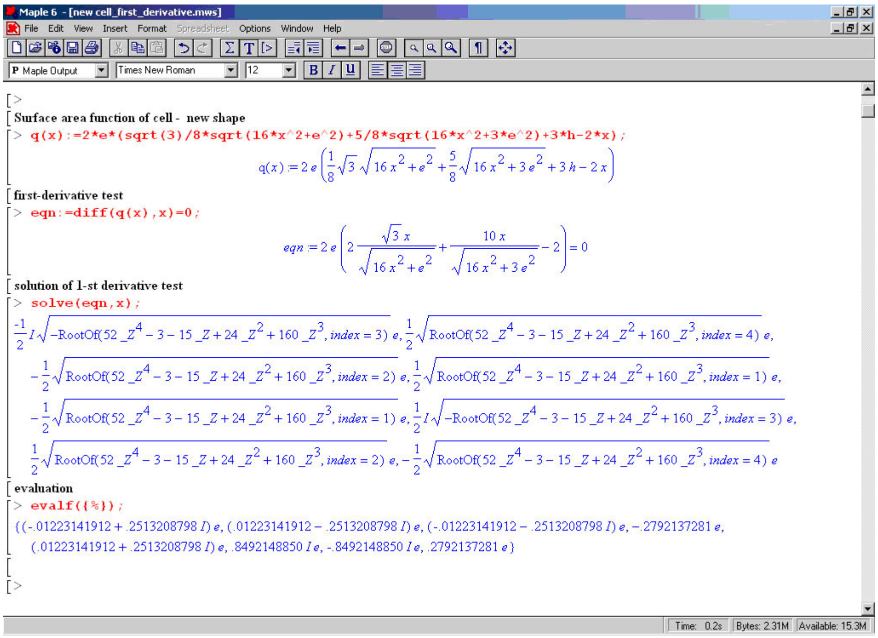

Figure 9: Calculation via a computer algebra system included in Maple®6.

We use the commands *eqn:= diff(q(x),x)=0; solve(eqn, x);* and *evalf(%)*. We observe that the solution contains eight roots, six of them are complex numbers and two are real.
The real roots are

$$x_{1,2} \doteq \pm 0.2792e \tag{34}$$

The second-derivative test is also performed through the software environment Maple®6. We call it through command *diff(q(x), x\$2)*. We obtain

$$q''(x) = 2e\left(\frac{-64\sqrt{3}x^2}{\sqrt{(16x^2+e^2)^3}} + \frac{4\sqrt{3}}{\sqrt{16x^2+e^2}} - \frac{160x^2}{\sqrt{(16x^2+3e^2)^3}} + \frac{10}{\sqrt{16x^2+3e^2}}\right). \tag{35}$$

Calling the command *simplify(diff(q(x), x\$2))* we get an expression which can be simplified manually into a more convenient form

$$q''(x) = e^3\frac{\sqrt{3}\left(32x^2+6e^2\right)\sqrt{16x^2+3e^2} + \left(240x^2+15e^2\right)\sqrt{16x^2+e^2}}{\sqrt{(16x^2+e^2)^3.(16x^2+3e^2)^3}}. \tag{36}$$

The function $q''(x)$ is positive for all real x. This implies that the function $q(x)$ has for $x_0 \doteq \pm 0.2792e$ minimum.

The internal angle $\angle MA_0N = \varphi$ is calculated from a tangent function in the right - angled triangle A_0NV. It holds true that

$$\tan\frac{\varphi}{2} = \frac{\frac{MN}{2}}{\frac{A_0P_0}{2}}. \tag{37}$$

Using (17) and (21), substituting $x_1 = 0.2792e$, we evaluate

$$\varphi \doteq 98.25°. \tag{38}$$

With reference to Fig.4 we evaluate the corresponding angle $\angle MA_0N$ in the truncated octahedron. Holds true that

$$\tan\frac{\psi}{2} = \frac{\frac{MN}{2}}{\frac{A_0P_0}{2}} = \frac{\frac{\sqrt{3}}{2}s}{\frac{\sqrt{2}}{2}s} = \sqrt{\frac{3}{2}} \doteq 1.2247 \tag{39}$$

From this implies that $\psi \doteq 101.53°$ and the model in Fig. 4 does not represent an optimal formation. As we mentioned above, in [2] proved that the surface-area of the model which arised by truncated octahedron is smaller than surface-area of the cell based on rhombic dodecahedron. Now, it would be interesting to compare the surface-areas of the cells which shapes are related to the extrema of the functions $p(x)$ and $q(x)$.

First, we compare the values of the functions. Using (7) and (34) we evaluate $p(x_0)$ and $q(x_1)$. By simplification

$$p(x_0) = \frac{3\sqrt{2}}{2}e + 6h \cdot e. \tag{40}$$

If in (34) for x_1 we substitute $x_1 = k.e$, $k = 0.2792$, then for holds true that

$$q(x_1) = \frac{e^2}{4} \cdot \left(\sqrt{48k^2+3} + 5.\sqrt{16k^2+3}\right) - 4k \cdot e^2 + 6h \cdot e. \tag{41}$$

From (40) and (41) implies that

$$\begin{aligned} q(x_1) &= e^2 \cdot \left(\frac{\sqrt{48k^2+3} + 5\sqrt{16k^2+3} - 6\sqrt{2}}{4}\right) - 4k \cdot e^2 + p(x_0) \\ &\vdots \\ q(x_1) &\doteq e^2 \cdot (1.1039 - 1.1168) + p(x_0) \end{aligned} \tag{42}$$

and holds true that $q(x_1) < p(x_0)$. One can see that the values e, h are not relevant in testing the models. In this extremal case the second model of the cell is the better-shaped open hexagonal structure with smaller surface-area then the first one. It is in conformity with the results in [2].

Using Maple®6 we plots the graphs of the functions $p(x)$ and $q(x)$ in Fig. 10.

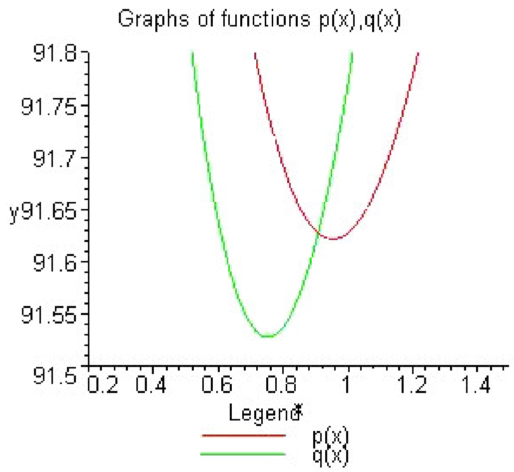

Figure 10: The graphs of functions $p(x)$ and $q(x)$ for arbitrary chosen parameters $e = 2.7$ and $h = 4.7$.

The visual juxtaposition can be provided by the usage of Cabri 3D.

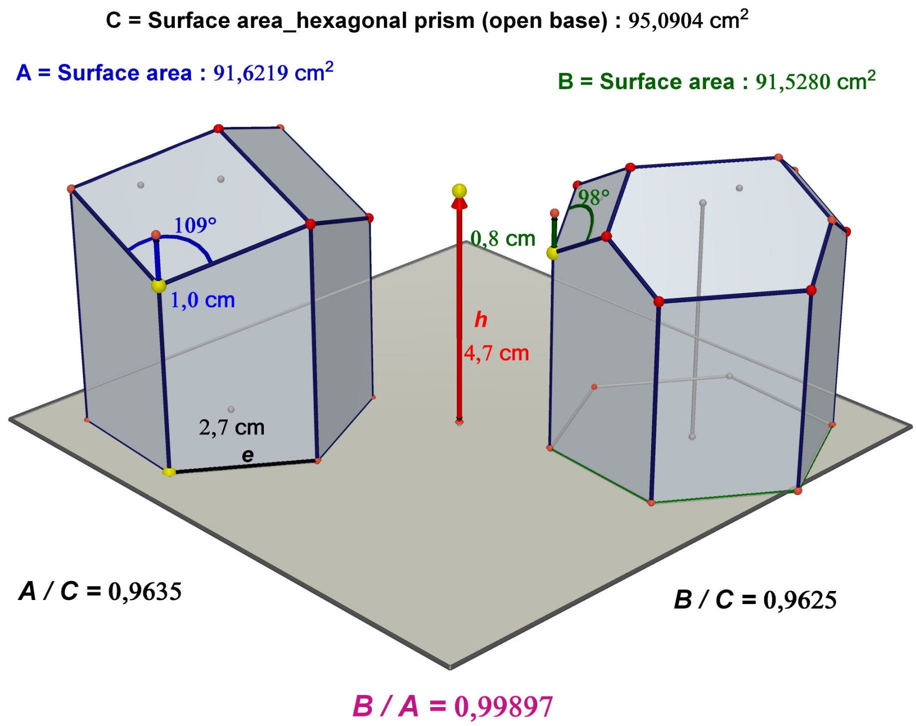

Figure 11: The parameters e, h are equal for these models. The values of x can be setting independently of each other and have a great influence on the calculations. One can observe that the extrema are dependent on the value of the angles. We note that the surface areas are calculated without the areas of hexagonal bases.

As we showed above, the function $q(x)$ describing the surface-area of this model. In the Fig. 11 is showed that the percentage difference in surface-area between the cell modeled with the bottom like the part of the rhombic dodecahedron and the modeled cell as the open hexagonal prism is 3.65%. The percentage difference between the cell modeled with the bottom like truncated octahedron and modeled cell as the open hexagonal prism is 3.75%. The percentage difference between the cell modeled with the bottom like the part of the rhombic dodecahedron and modeled cell with the bottom like truncated octahedron is 0.11%.

3 Conclusion - a note to real experimental data

There are about 30 subspecies and many more hybrids of bees in the world and their parameters e, h are different, e.g. in [19] there is a specified range $e \doteq 2.82$mm -2.94mm. We have already mentioned above that the values e, h are not relevant in testing the model. What is critical is the internal angle of the rhombus and, indeed, the experimental value of the internal angle of rhombus is approximately $109°$. It means that the mathematical model whose surface-area is described by the function $p\left(x\right)$ is in accordance with the natural design of the bee cell.
The second model whose surface-area is described by the function $q\left(x\right)$ was discovered by the famous mathematician Laszlo Fejes-Toth. In his article he solved the difficult problem of how to tessellate the space between two planes with convex congruent polyhedra satisfying two conditions while minimizing the surface area with regard to the occupied volume. [2]
Due to complexity of the function $q\left(x\right)$, we used software to determine its extreme. In Fig. 12, one can see some cells which have their bottoms built from hexagons and rhombi. For these cells, it is typical to have a clearly visible segment at the bottom instead of a single point. The existence of such a type is unusual and also contrary to Fejes-Toth, who claims the bees use the three rhombi model consistently.

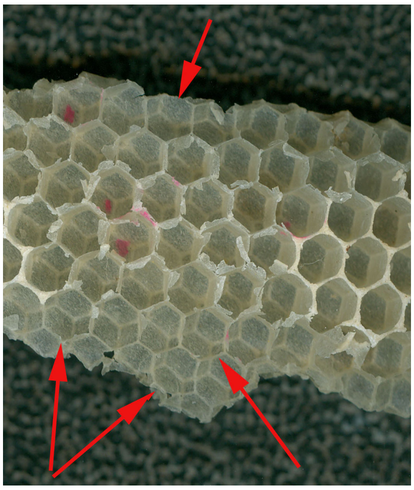

Figure 12: Photograph of a natural honeycomb with special bottom cells. As the arrows indicate, some bottoms are built from hexagons and rhombi.

It is true that mathematical models are ideals and the real bee cell is a crude approximation of a pure geometric shape. A lot of beekeeping experts consider that the bees build cylindrical cells from wax first. Later, they heat the wax and the surface tension remoulds these shapes into an appropriate optimal design. This could be the reason why one can find both types of the models on the edge of the natural honeycombs. However, these assumptions should be supported by serious research. We are not aware that such research has been realized yet. Therefore it is not possible to compare mathematically derived results with practice.

Acknowledgement
We would like to thank the reviewers whose comments and suggestions very much helped to improve and clarify this manuscript. Our special thanks belong to Dalibor Titěra, a researcher from the Bee Research Institute at Dol, Czech Republic, for his advice on the specific problems of beekeeping and biology of bees.

References

[1] Hope - Jones, W., 1936: The Rhombic Dodecahedron for the Young. *Mathematical Gazette*, **20**, 254-257.

[2] Fejes-Toth, L., 1964: What the bees know and what they do not knot. *Bull. Amer Math. Soc.*, **70**, 468-481.

[3] Heath, T. A., 1981: *History of Greek Mathematics*. Dover Publications, Inc., 461 pp.

[4] Gay, D., 1998: *Geometry by discovery*. John Wiley and Sons. Inc., 410 pp.

[5] Dimitric, R. M., 2001: Using less calculus in teaching: An Historical Approach. *Mathematics Magazine*, **74**, 201-211.

[6] Devlin, K., 2002: *The Language of Mathematic: Making the Invisible Visible*. Freeman and Company, 412 pp.

[7] Hilbert, D. and S. Cohn-Vossen, 1999: *Geometry and the Imagination.* AMS Chelsea Pub., 357 pp.

[8] Thompson, D. A . W., 1945: *On growth and form*. Cambridge University Press, 1098 pp.

[9] Niven, I., 1981: *Maxima and Minima Without Calculus*. MAA, 303 pp.

[10] Miéwis, N., 2009: De wiskunde van de honingbij. [The mathematics of the honey bee]. *Uitwiiskeling*, **25**, 4-14. Dutch.

[11] Svoboda, J., 1887: Geometrie včel. [Geometry of Bees]. *Časopis pro pěstovaní matematiky a physiky*, **72**, 85-90. Czech.

[12] Polachek, H., 1940: The structure of the honeycomb. *Scripta Math.*, **7**, 87-98.

[13] Ball, P., 2009: *Nature's Patterns: A Tapestry in Three Parts*. Oxford University Press, 320 pp.

[14] Roberts, W J., 1984: Honeycomb geometry: Applied Mathematics in nature. *Mathematics Teacher*, **77**, 188-190.

[15] Molitor, J., 1987: The honeycomb of bees. *Prax. Mathematics*, **29**, 333-336.

[16] Faigle, E., 1988: Bienen sparen beim Wabenbau Material. [Bees save material for honeycomb construction].*Mathematische Unterricht*, **9**, 37- 44. German.

[17] Sharp, B., 2008: Getting a bee in mathematics class. *Mathematics Teacher*, **14**, 182-189.

[18] Hargittai, I. and M. Hargittai, 1994: *Symmetry: A unifying concept.* Shelter, 222 pp.

[19] Peacock, P., 2008: *Keeping bees: A complete practical guide*. Octopus Pub., 144 pp.

[20] Shah, P. and A. Miyake, 2005: *The Cambridge handbook of Visuospatial Thinking*, Cambridge University Press, 579 pp.

[21] Wentworth, G. and D. E. Smith, 1913: *Solid Geometry*. The Atheneum Press, 218 pp.

[22] Hašek, R., 2012: Investigation of logarithmic spirals in nature by means of dynamic geometry and computer algebra systems. *The Electronic Journal of Mathematics and Technology*, **6**, 216-230.

[23] Bolt, B., 1991: *Mathematics meets Technology*. Cambridge University Press, 214 pp.

[24] Vidermanova, K., A. Viziova and J. Zahorska, 2012: Analyza ziackych chyb pri konstrukcii rezov telies a moznosti ich odstranenia vyuzitim programu Cabri 3D. [Analysis of students mistakes in solution of the sections of solids and using of Cabri 3D for their removing]. Proc. Acta Mathematica 15, X. Mathematics Conference in Nitra, Nitra, Slovakia, FNS CPU in Nitra, 179 -189 [Available from: http://www.nmk.fpv.ukf.sk/2012/proceedings.php]

[25] Benacka, J., 2012: Cutting solid figures by plane analytical solution and spreadsheet implementation. *International Journal of Mathematical Education in Science and Technology*, **43**, 647-654.

[26] Benacka, J., 2007: Spreadsheet numerical modelling in secondary school physics and biology. *Spreadsheets in education (eJSiE)* , **2**, 289 - 298.

[27] Cundy, H. M. and A. P. Rollett, 1981: *Mathematical Models*. Tarquin Pub., 286 pp.

[28] Cabrilog, 2006: Cabri 3D vesion v 2. [Available online at http://www.cabri.com]